Reinstatement of nicotine seeking is mediated by glutamatergic plasticity

Cassandra D. Gipson[1], Kathryn J. Reissner, Yonatan M. Kupchik, Alexander C. W. Smith, Neringa Stankeviciute, Megan E. Hensley-Simon, and Peter W. Kalivas[1]

Department of Neurosciences, Medical University of South Carolina, Charleston, SC 29425

Edited by Jean-Pierre Changeux, Institut Pasteur, Paris Cedex 15, France, and approved April 10, 2013 (received for review December 1, 2012)

Nicotine abuse and addiction is a major health liability. Nicotine, an active alkaloid in tobacco, is self-administered by animals and produces cellular adaptations in brain regions associated with drug reward, such as the nucleus accumbens. However, it is unknown whether, akin to illicit drugs of abuse such as cocaine or heroin, the adaptations endure and contribute to the propensity to relapse after discontinuing nicotine use. Using a rat model of cue-induced relapse, we made morphological and electrophysiological measures of synaptic plasticity, as well as quantified glutamate overflow, in the accumbens after 2 wk of withdrawal with extinction training. We found an enduring basal increase in dendritic spine head diameter and in the ratio of AMPA to NMDA currents in accumbens spiny neurons compared with yoked saline animals at 2 wk after the last nicotine self-administration session. This synaptic potentiation was associated with an increase in both AMPA (GluA1) and NMDA (GluN2A and GluN2B) receptor subunits, and a reduction in the glutamate transporter-1 (GLT-1). When nicotine seeking was reinstated by presentation of conditioned cues, there were parallel increases in behavioral responding, extracellular glutamate, and further increases in dendritic spine head diameter and ratio of AMPA to NMDA currents within 15 min. These findings suggest that targeting glutamate transmission might inhibit cue-induced nicotine seeking. In support of this hypothesis, we found that pharmacological inhibition of GluN2A with 3-Chloro-4-fluoro-N-[4-[[2-(phenylcarbonyl)hydrazino]carbonyl]benzyl]benzenesulfonamide (TCN-201) or GluN2B with ifenprodil abolished reinstated nicotine seeking. These results indicate that up-regulated GluN2A, GluN2B, and rapid synaptic potentiation in the accumbens contribute to cue-induced relapse to nicotine use.

Tobacco smoking is the leading preventable cause of mortality, and relapse rates remain high (1, 2). Nicotine is a primary active alkaloid in tobacco and is generally recognized as being responsible for maintaining smoking behavior in humans (3). Accordingly, current smoking pharmacotherapy relies largely on replacing nicotinic receptor stimulation with compounds having pharmacokinetic and/or receptor efficacy characteristics that decrease nicotine craving without producing significant reward (4). Given the high rates of failure by replacement therapies, there is a pressing need to develop effective new medications targeting the neurological changes produced by cigarette use that underpin persistent relapse vulnerability.

Nicotine self-administration results from activating $\alpha_4\beta_2$ subunit-containing nicotinic cholinergic receptors localized on dopamine cell bodies in the ventral tegmental area and by stimulating presynaptic α_7-containing nicotinic acetylcholine receptors on glutamatergic afferents to dopamine neurons (5–7); the net consequence being increased dopamine release in the nucleus accumbens, a brain nucleus central to reward circuitry (8). In contrast to the well-understood synaptic physiology mediating the reinforcing properties of nicotine administration, the neuroadaptations underlying the enduring vulnerability to relapse produced by continued nicotine use are largely unknown. Studies examining brain tissue within 24 h after discontinuing nicotine self-administration reveal decreased accumbens proteins involved in glutamate signaling (9), including glial glutamate transport and presynaptic, release-regulating mGluR2/3 receptors (10). Thus, akin to other addictive drugs, such as cocaine, heroin, and alcohol, the enduring susceptibility to relapse to nicotine use may involve changes in accumbens glutamate transmission. However, it remains unexplored whether the nicotine-induced glutamatergic adaptations endure after more extended withdrawal, and whether they are required for nicotine relapse. For example, it is unclear whether rats withdrawn from nicotine self-administration share characteristics of altered spine morphology and synaptic strength seen after chronic cocaine or heroin administration (11, 12), or whether reinstating nicotine seeking further alters synaptic plasticity. Similarly, it is unknown whether there are enduring changes in extracellular glutamate as with withdrawal from cocaine (13) or in the glutamate receptors and transporters that regulate synaptic strength. Here we demonstrate that 2 wk after discontinuing nicotine self-administration there are enduring changes in glutamatergic synaptic physiology and morphology in the accumbens akin to what is produced by cocaine self-administration, and that further changes are elicited during cue-induced reinstatement of nicotine seeking [animal model of relapse (14)]. These changes in synaptic plasticity are associated with elevations in glutamate receptor subunits, and inhibiting GluN2A- or GluN2B-containing NMDA receptors abolished reinstated nicotine seeking.

Results

Cue-Induced Nicotine Seeking in Rats Extinguished from Nicotine Self-Administration. We used an i.v. nicotine self-administration protocol that paired cues with nicotine infusion. The protocol used is outlined in Fig. 1*A*, which shows the pattern of nicotine self-administration and extinction from all animals used in this study. Rats were trained to self-administer nicotine for 2 wk with a compound stimulus (light + tone cues) delivered with each nicotine infusion and were placed into extinction training without cues for another 14 d (Fig. 1*B*). Rats were given a reinstatement trial on day 29, which consisted of pressing the active lever for delivery of the light/tone cue. Animals showed a marked reinstatement of lever pressing on the nicotine-paired (active) lever [Fig. 1*C*; Time: $F_{(6,47)} = 24.83$, $P < 0.001$; Lever: $F_{(1,47)} = 272.41$, $P < 0.001$; Interaction: $F_{(6,47)} = 33.37$, $P < 0.001$].

Relapse to Nicotine Seeking Is Associated with Increased Glutamate Release in the Core Subcompartment of the Nucleus Accumbens. Previous studies with cocaine and heroin, but not sucrose, self-administration show that reinstating lever pressing is associated with an increase in extracellular glutamate in the core subcompartment of the nucleus accumbens (NAcore) (15). The

Author contributions: C.D.G. and P.W.K. designed research; C.D.G., K.J.R., Y.M.K., A.C.W.S., N.S., and M.E.H.-S. performed research; C.D.G. and P.W.K. analyzed data; and C.D.G. and P.W.K. wrote the paper.

The authors declare no conflict of interest.

This article is a PNAS Direct Submission.

[1]To whom correspondence may be addressed. E-mail: gipson@musc.edu or kalivasp@musc.edu.

This article contains supporting information online at www.pnas.org/lookup/suppl/doi:10.1073/pnas.1220591110/-/DCSupplemental.

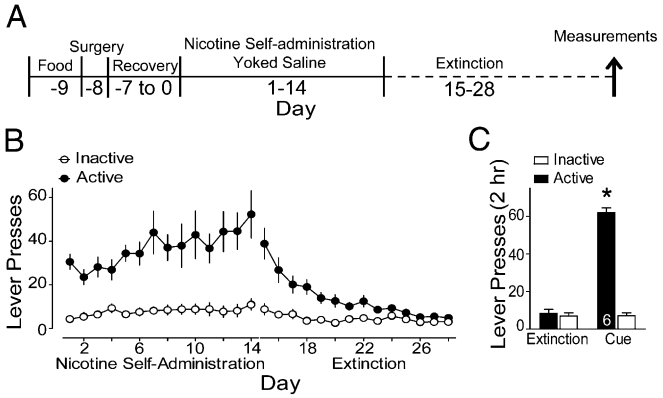

Fig. 1. Nicotine self-administration and reinstatement of nicotine-seeking behavior. (*A*) Nicotine self-administration and extinction training before reinstatement testing and measurements for either d_h, A/N, microdialysis, or Western blot analysis. (*B*) Rats acquired lever responding to the active lever to receive i.v. infusions of nicotine (0.02 mg/kg per infusion). During extinction training, active lever presses decreased to inactive lever press rates. (*C*) Restoration of the conditioned cues to the active lever significantly reinstated lever pressing in animals given 120-min reinstatement of cue-induced nicotine seeking. $^*P < 0.05$, comparing active lever pressing after cues with extinction pressing (average of the last three extinction sessions).

reinstatement-associated increase in extracellular glutamate is derived from prefrontal cortical afferents (13, 16). Fig. 2 *A–C* shows that cue-induced reinstatement of nicotine seeking also produced an increase in extracellular glutamate in the NAcore during the first 40 min [Time $F_{(11,11)} = 2.76$, $P < 0.01$; Treatment $F_{(1,11)} = 7.88$, $P < 0.01$; Interaction $F_{(11,165)} = 2.12$, $P < 0.01$]. In yoked saline animals, cue presentation did not elicit either an increase in active lever pressing or extracellular glutamate. The levels of glutamate were normalized to percent change from baseline because the basal levels of glutamate did not differ between treatment groups (Saline = 34.2 ± 9.8 pmol/sample, $n = 9$; Nicotine = 37.9 ± 9.7, $n = 8$). Fig. 2*D* shows that all dialysis probes passed through the dorsoventral extent of the NAcore, with portions of the active membrane also in striatum dorsal to the NAcore and/or the ventral shell subcompartment of the accumbens.

Rapid Synaptic Potentiation During Nicotine Reinstatement. Presynaptic and nonsynaptic glutamate release regulates synaptic plasticity in both primary cell cultures and in vivo (17, 18). Accordingly it is possible that the rapid cue-induced elevation in extracellular glutamate seen during reinstated nicotine seeking may produce parallel synaptic plasticity. Synaptic potentiation is associated with an increase in dendritic spine head diameter (d_h) and an increase in the ratio of AMPA to NMDA current (A/N) (19–21). Accordingly, we obtained measures of spine morphology and AMPA and NMDA glutamate receptor-mediated currents at 15 min after inducing reinstatement of nicotine seeking with the light/tone cue. To quantify spine density and d_h, 3D confocal images were made of neurons in the NAcore that were diolistically labeled with the lipophilic dye DiI (Fig. 3 *A* and *B*) (11), and AMPA and NMDA receptor-mediated currents were quantified using whole-cell patch recordings from medium spiny neurons (MSNs) in NAcore tissue slices (Fig. 4) (11, 17). To assess both stable changes in synaptic plasticity induced by withdrawal from nicotine self-administration and transient reinstatement-induced changes, d_h, spine density, and A/N were quantified just before beginning cue-induced reinstatement (time $t = 0$), or at 15 min ($t = 15$) or 45 min ($t = 45$) after beginning the reinstatement trial. Fig. 3*C* shows significant increases in active lever pressing induced by cues in both the $t = 15$ and $t = 45$ treatment groups, and that the increase occurred almost entirely during the first 15 min after initiating the reinstatement session.

Spine morphology. After 2 wk of extinction training (day 36, Fig. 1*A*), d_h was significantly elevated in the nicotine group (0.436 ± 0.009 μm, mean ± SEM) compared with yoked saline animals (0.334 ± 0.004 μm) [Fig. 3*D*; one-way ANOVA, group: $F_{(5,232)} = 87.26$, $P < 0.001$]. The increase in spine diameter is also apparent in the cumulative distribution of d_h in Fig. 3*E* that shows a shift to the right in the $t = 0$ nicotine group compared with the saline rats [two-way ANOVA, group: $F_{(5,1464)} = 74.93$, $P < 0.001$; d_h: $F_{(5,1464)} = 9176.00$, $P < 0.001$; interaction: $F_{(25,1464)} = 21.64$, $P < 0.001$]. In contrast to d_h, there was no difference in spine density at $t = 0$ between nicotine and saline rats (Fig. 3*F*). When spine morphology was examined at 15 and 45 min after initiating reinstatement, d_h measured as mean or cumulative distribution was further increased at $t = 15$ min (0.484 ± 0.006 μm) and returned to nicotine baseline levels by $t = 45$ min (0.410 ± 0.006 μm) (Fig. 3 *D* and *E*). No change in spine density was measured at any time point (Fig. 3*F*).

Synaptic currents. Using whole-cell patch-clamp recordings, we found changes in A/N that paralleled those in d_h. After extinction training in the absence of cues ($t = 0$) the A/N was significantly elevated in the nicotine (1.52 ± 0.08) compared with yoked saline animals (1.12 ± 0.10) (Fig. 4*A*). At 15 min after initiating cue-induced reinstatement, the A/N further increased

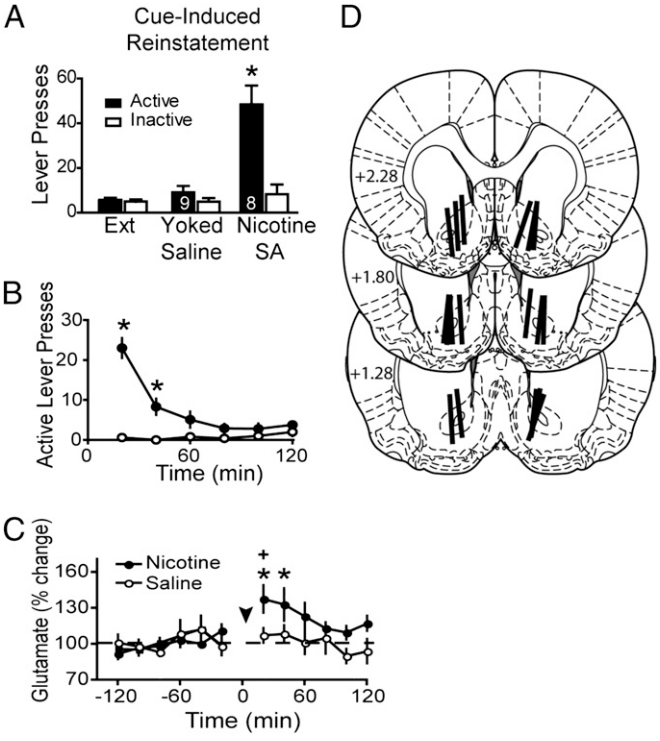

Fig. 2. Increased extracellular glutamate in the NAcore during cue-induced reinstatement of nicotine seeking. (*A*) The delivery of conditioned cues induced significant active lever pressing in nicotine-experienced animals, whereas the same cues in yoked saline animals did not alter behavior. (*B*) Time course of reinstated nicotine seeking revealed increased active lever pressing during the first 40 min after initiating the reinstatement session. (*C*) Reinstatement of nicotine seeking increased extracellular glutamate levels during the first 40 min after beginning cue-induced reinstatement. Arrowhead refers to initiation of cue-induced reinstatement session. (*D*) Histological verification of guide cannula placement according to Paxinos and Watson (2007) (41) by an individual unaware of the animal's treatment group. Numbers refer to mm rostral to Bregma. $^*P < 0.05$ compared with extinction active lever pressing in *A*, yoked saline in *B*, or basal glutamate in *C*. $^+P < 0.05$ comparing nicotine with saline.

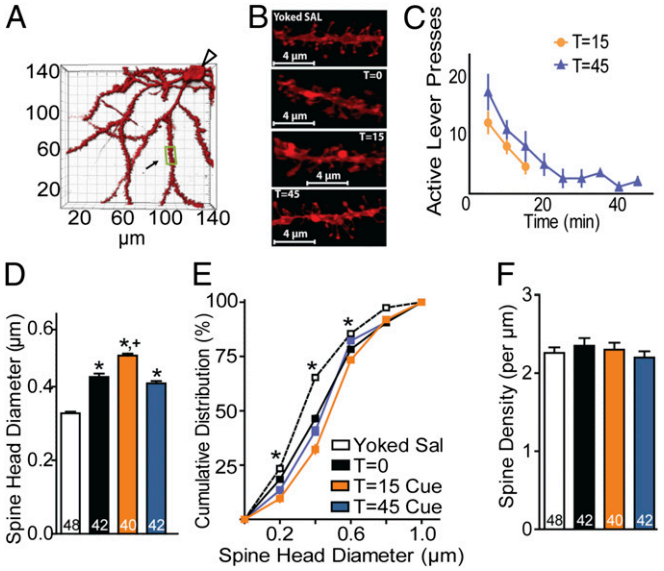

Fig. 3. Nicotine seeking enlarges NAcore spine head diameter. (*A*) Example of a high-resolution 3D reconstruction of an NAcore MSN. Clear arrow, location of soma; boxed region, segment analyzed in *B* from a $t = 45$ animal. (*B*) Sample dendrites from NAcore spiny cells in yoked saline ($d_h = 0.342$ μm) or cocaine-trained rats at $t = 0$ (0.423 μm), $t = 15$ cue (0.495 μm), and $t = 45$ cue (0.418 μm) after initiating cue-induced reinstatement. (*C*) Time course of reinstated active lever pressing in the $t = 15$ min and $t = 45$ min groups. (*D*) Mean d_h was increased after withdrawal from nicotine self-administration ($t = 0$) and was further increased at $t = 15$ by contingent conditioned cues. (*E*) Cumulative d_h frequency plot indicating a rightward shift at $t = 0$ compared with saline and a further rightward shift at $t = 15$ min after cue. By $t = 45$ min after cue the cumulative d_h distribution had returned to $t = 0$ min. (*F*) No difference in spine density was found between groups. $^*P < 0.05$ compared with yoked saline animals; $^+P < 0.05$ compared with $t = 0$.

[1.90 ± 0.09; one-way ANOVA, $F_{(2,33)} = 17.94$, $P < 0.001$]. In addition to A/N, we quantified the time required for the NMDA current to decay to 37% of its peak current, and Fig. 4*B* shows that nicotine-trained animals (292.8 ± 11.7 ms) had increased NMDA decay times compared with yoked saline rats (244.6 ± 8.9 ms) at $t = 0$, but unlike the A/N, the decay time did not increase further at $t = 15$ min [313.2 ± 19.4 ms; one-way ANOVA, $F_{(2,31)} = 6.57$, $P < 0.01$].

Nicotine Self-Administration Changes Expression of Proteins Regulating Glutamatergic Signaling. The glutamate overflow measured during reinstated nicotine seeking could arise from reduced elimination of extracellular glutamate by membrane-bound glial glutamate transporters (GLT-1) (22). To examine this possibility, we used Western blotting to quantify the membrane content of GLT-1 in the NAcore. In line with prediction, we observed a significant reduction in the levels of GLT-1 [$t_{(24)} = 1.86$, $P < 0.05$; Fig. 5*A*] but no change was measured in the glial glutamate aspartate transporter (GLAST). Moreover, a higher AMPA current as shown in Fig. 4*A* is often associated with increases in the GluA1 AMPA subunit (23, 24), and we found that the membrane level of GluA1 was significantly elevated in the NAcore of $t = 0$ nicotine compared with yoked saline [$t_{(11)} = 1.91$, $P < 0.01$]. The increase in GluA1 was not associated with a parallel increase in the GluA2 subunit, potentially indicating that the increase in AMPA receptors was largely GluA2-lacking receptors. GluA2-lacking receptors are also up-regulated after chronic use of cocaine (24). A slower decay of the NMDA current as shown in Fig. 4*B* can indicate elevated expression of GluN2B receptors (11, 25), and we found that GluN2B was elevated in $t = 0$ nicotine animals compared with yoked saline [$t_{(12)} = 3.70$, $P < 0.05$]. The increase in GluN2B was accompanied by a parallel increase in GluN2A [$t_{(11)} = 2.22$, $P < 0.05$].

Nicotine Reinstatement Is Prevented by Pharmacological Inhibition of GluN2A and GluN2B. Up-regulation of GluN2A in NAcore after extinction training from nicotine self-administration indicates an increase in synaptic NMDA receptors (26), which could contribute to the reinstated nicotine seeking initiated by increased extracellular glutamate observed in Fig. 2. To determine whether NAcore GluN2A receptors are important in cue-induced nicotine seeking, the GluN2A antagonist 3-Chloro-4-fluoro-N-[4-[[2-(phenylcarbonyl)hydrazino]carbonyl]benzyl]benzenesulfonamide (TCN-201) was microinjected into NAcore (0.01 and 0.1 nmol). Both doses of TCN-201 decreased cue-induced nicotine seeking compared with artificial cerebrospinal fluid (aCSF) vehicle [Fig. 5*B*; $F_{(7,77)} = 43.05$, $P < 0.001$]. To determine whether the attenuated lever pressing was due to sedation, locomotor activity was examined in a novel open field after NAcore injection. No difference in open field locomotor activity was found between vehicle and 0.1 nmol TCN-201 (Fig. S1).

The elevation in GluN2B may indicate an increase in extrasynaptic NMDA receptors because many studies show preferential distribution of GluN2B outside of the synaptic cleft (26, 27), and newly inserted GluN2B receptors are known to be involved in synaptic plasticity induced by drugs of abuse (28). The elevated extrasynaptic glutamate level during cue-induced reinstatement of nicotine seeking (Fig. 2) would be predicted to stimulate the up-regulated GluN2B (Fig. 5*A*) in nicotine-withdrawn animals, which in turn could drive reinstated nicotine seeking. To determine whether this sequence of events may contribute to reinstated nicotine seeking, we pretreated animals systemically with doses of the GluN2B antagonist ifenprodil (29) and do not alter locomotor activity (11). Fig. 5*C* shows that compared with injection of water vehicle, ifenprodil abolished cue-induced reinstatement at a dose of 3 mg/kg, i.p., and partly antagonized reinstatement at 1 mg/kg, i.p. [$F_{(7,95)} = 23.90$, $P < 0.001$].

Discussion

Our results show that after withdrawal from nicotine self-administration excitatory synapses in the NAcore were resting in a relatively potentiated state, as indicated by increases in d_h and A/N. In accord with this physiological adaptation, levels of AMPA and NMDA receptor subunits were also elevated. Consistent with the

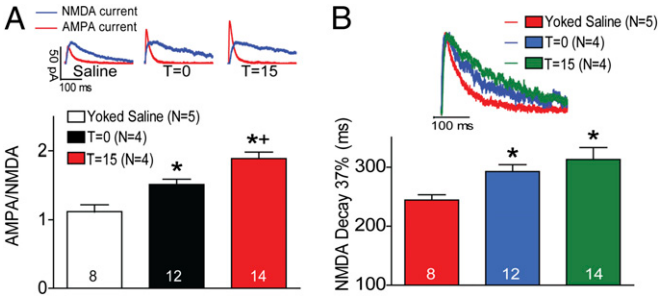

Fig. 4. Rapid increase in A/N during cue-induced reinstatement of nicotine seeking. (*A*) Sample AMPA and NMDA current traces from each group. A/N was significantly elevated in animals withdrawn with extinction training from nicotine self-administration compared with yoked saline animals. The initiation of cue-induced reinstatement of nicotine-seeking further elevated A/N at $t = 15$. (*B*) Decay time (time to 37% decay) for NMDA currents in nicotine-extinguished animals was significantly increased in nicotine-extinguished animals ($t = 0$) as well as animals at $t =$ min compared with yoked saline animals. N in parentheses is number of animals. The number in bars is number of cells recorded in each condition. $^*P < 0.05$ compared with yoked saline animals at $t = 0$ (white bar); $^+P < 0.05$ compared with $t = 0$.

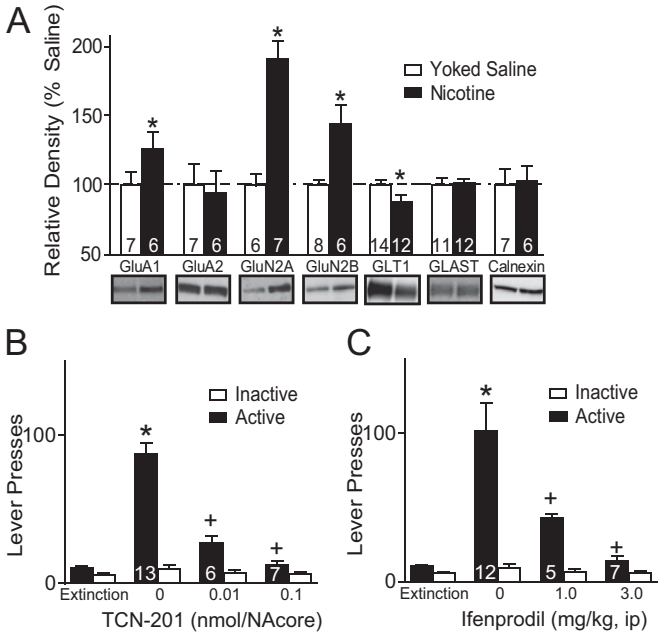

Fig. 5. Increased GluN2A- and GluN2B-containing NMDA receptors mediate cue-induced nicotine reinstatement. (*A*) Withdrawal from nicotine self-administration (t = 0) significantly elevated membrane-bound GluA1, GluN2A, and GluN2B and reduced GLT1 in the NAcore compared with yoked saline. All data were normalized to calnexin as a loading control. (*B*) Intra-NAcore injection of the GluN2A antagonist TCN-201 reduced cue-induced nicotine seeking. (*C*) Systemic injection of the GluN2B antagonist ifenprodil produced a dose-dependent reduction in cue-induced reinstated nicotine seeking. $^{*}P < 0.05$ compared with either yoked saline (white bar) or extinction active lever presses; $^{+}P < 0.05$ compared with vehicle active lever presses.

fact that nicotine has been classified as a psychostimulant (30), this long term potentiation (LTP)-like state after self-administered nicotine is similar to what is produced by cocaine self-administration (17, 24) but opposite to that elicited by heroin self-administration (11). Although differential effects on resting synaptic strength in the NAcore between psychostimulants and heroin would seem to support different underlying mechanisms of relapse vulnerability (31), we also found that reinstating nicotine seeking with conditioned cues elicits glutamate overflow in the NAcore akin to what is seen during heroin, alcohol, and cocaine reinstatement (13, 15, 32). Furthermore, the glutamate overflow was associated with rapid, transient synaptic plasticity as illustrated by cue-induced increases in d_h and A/N, and this rapid synaptic plasticity is also produced during cocaine or heroin reinstatement (11, 33). Thus, although resting synaptic strength at excitatory synapses in NAcore may differ markedly depending on which addictive drug is self-administered, when an animal is presented with conditioned cues or the drug itself, rapid synaptic potentiation is induced regardless of whether animals had self-administered nicotine, cocaine, or heroin.

We measured relevant proteins that could mediate the effects of nicotine self-administration to potentiate glutamate overflow, A/N, and d_h during cue reinstatement. Glutamate overflow was associated with reduced levels of glutamate elimination from the synaptic cleft, as indicated by decreased content of the glial glutamate transporter GLT-1. Reduced protein content of GLT-1 is also seen after withdrawal from cocaine self-administration, and restoration of GLT-1 by ceftriaxone or *N*-acetylcysteine inhibits reinstated cocaine, nicotine, heroin, and alcohol seeking (22, 34–36). Akin to cocaine-withdrawn rats (24), the increase in A/N after nicotine withdrawal was associated with elevated levels of GluA1. Although these LTP-like changes in AMPA receptors differ from heroin withdrawal, akin to heroin, nicotine withdrawal was associated with increased GluN2B-containing NMDA receptors (11). Unique to nicotine, both the GluN2A and GluN2B subunits were elevated. Importantly, selectively blocking either GluN2A- or GluN2B-containing NMDA receptors prevented reinstated nicotine seeking. Many studies indicate that in adult GluN2A-containing receptors are mostly located in the synaptic cleft (26), whereas GluN2B receptors are proportionally in higher density in the extrasynaptic space (37). Thus, any increase in GluN2A signaling accompanying nicotine up-regulated protein would occur regardless of glutamate spillover from the synaptic cleft. In contrast, stimulation of GluN2B may occur primarily during the synaptic spillover of glutamate in the NAcore that accompanies cue-induced nicotine seeking. Because blocking GluN2B receptors prevented reinstated nicotine seeking, this may be an important mechanism for initiating reinstatement. Indeed, stimulation of GluN2B receptors is known to promote LTP-like postsynaptic increases in AMPA receptors and currents (38), and blocking GluN2B, but not GluN2A, also inhibits heroin-induced reinstatement (11). Together, these findings support a scenario whereby reduced elimination of synaptically released glutamate via down-regulated GLT-1 increases synaptic glutamate overflow (Fig. 2) and increases stimulation of extrasynaptic GluN2B-containing receptors that promotes both LTP and reinstatement. Stimulation of either NMDA receptor subtype involves calcium influx that could promote the LTP-like changes accompanying nicotine reinstatement (38). This is consistent with previous findings that the increase in surface AMPA receptors in the accumbens shell 30 min after initiating cocaine reinstatement is calcium/calmodulin-dependent protein kinase II (CaMKII)-dependent (39).

In summary, our data demonstrate a glutamatergic mechanism in the NAcore that contributes to the vulnerability to relapse to nicotine seeking. Specifically, we found a cocaine-like increase in synaptic strength and d_h in rats withdrawn from nicotine self-administration. It will be of interest in future studies to determine whether the changes identified here are selective for D1 or D2 receptor expressing MSNs, although it seems that D1-expressing MSNs may be of particular importance after cocaine administration (40). Akin to both cocaine and heroin, this LTP-like state was potentiated during cue-induced reinstatement and associated with an increase in extracellular glutamate. Finally, blocking either GluN2A- or GluN2B-containing NMDA receptors prevented reinstated nicotine seeking. Nicotine has well-characterized binding sites in brain that are distinct from cocaine and heroin, yet our data indicate that relapse to all three classes of addictive drug share certain glutamatergic adaptations. Thus, our findings support a hypothesis that certain changes in prefrontal cortex glutamatergic regulation of NAcore are shared between addictive drugs and contribute to the enduring relapse vulnerability that is emblematic of all substance abuse disorders.

Experimental Procedures

Animal Housing and Surgery. Male Sprague-Dawley rats (250 g; Charles River Laboratories) were individually housed with a 12-h/12-h dark/light cycle. All experimentation occurred in the dark cycle. Rats received food ad libitum until the day before behavioral training, after which food restriction (20 g of rat chow per day) was implemented and maintained throughout the experiment. Rats were allowed 1 wk to acclimate to the vivarium before inducing anesthesia and implanting indwelling jugular catheters. All procedures were in accordance with the National Institutes of Health Guide for the Care and Use of Laboratory Animals and the Assessment and Accreditation of Laboratory Animal Care.

Nicotine Self-Administration and Reinstatement Procedures. After acclimation to facilities, male Sprague-Dawley rats underwent one overnight food-training session, followed by in-dwelling jugular catheterization surgery. After recovery, animals begin daily 2-h nicotine self-administration sessions, in which one response on the active lever yielded one i.v. nicotine infusion (0.02 mg/kg/infusion), paired with two white cue lights above both the active

and inactive lever and a discrete tone cue (2,900-Hz tone). An inactive lever was available throughout the duration of each session to control for nonspecific responding. After 14 consecutive sessions of self-administration (≥10 infusions per day), rats were placed into daily extinction training sessions (no nicotine delivery or cues) for at least 14 sessions, or until extinction criteria were met (≤25 active lever responses for a minimum of two sessions). Reinstatement was elicited by cues (tone + light delivery after an active lever press). Food-trained yoked saline controls were used as a comparison group. For the ifenprodil experiment, animals were withdrawn from nicotine self-administration and given 120 min cue-induced reinstatement test after injection. Animals were allowed to reextinguish active lever responding between reinstatement test sessions. Ifenprodil dose–response was generated such that each animal received both vehicle and one dose of ifenprodil, either 1.0 or 3.0 mg/kg, in a randomized order. TCN-201 dose–response was generated such that each animal received both vehicle and one dose of TCN-201 in a randomized order.

Microdialysis, Microinjection Procedures, and Histology. For microdialysis, in-house probe construction procedures and aCSF content are described elsewhere (15). The night before collecting samples, the probes were inserted into the accumbens and perfused with aCSF (0.2 μL/min). Flow rate was increased to 2.0 μL/min the following morning, 2 h before baseline collection. Six baseline collections were then taken in 20-min intervals. Immediately before sample 7, levers were extended for a 2-h cue reinstatement session. Dialysate samples were stored at −80 °C before being analyzed for glutamate using HPLC with electrochemical detection (*SI Experimental Procedures*). For microinjections, rats were stereotaxically implanted immediately after catheterization with bilateral guide cannulae aimed above NAcore (details in *SI Experimental Procedures*). Obturators were placed into the guide cannulae during the experimental protocol to prevent outside debris from entering the cannulae and were removed during microinfusions. Bilateral injection cannulae were lowered, and 0.5 μL TCN-201 (0, 0.01, or 0.1 nmol) was infused using a syringe pump. Rats were placed in the operant chamber for cue reinstatement 15 min after removal of injection cannulae. Obturators were again placed in the guides after injection. Coronal slices (100 μm thick) of NAcore were mounted and stained via cresyl violet to verify guide cannulae placement (Fig. S1).

Quantification of Dendritic Spines. A confocal microscope (Zeiss LSM 510) was used to image DiI-labeled sections, and DiI was excited using the Helium/Neon 543-nm laser line. The micrograph of DiI-labeled dendrite (Fig. 1*C*) was acquired via optical sectioning by a 63× oil immersion objective (Plan-Apochromat, Zeiss; N.A. = 1.4, working distance = 90 μm) with pixel size 0.07 μm at XY plane and 0.1-μm intervals along the *z* axis. Images were deconvoluted by Autoquant before analysis (Media Cybernetics), and then a 3D perspective was rendered by the Surpass module of the Imaris software package (Bitplane). Only spines on dendrites beginning at >75 μm and ending at ≤200 μm distal to the soma and after the first branch point were quantified from cells localized to the NAcore. The length of quantified dendrites was 45–55 μm. For each of the animals examined in each group, 5–12 neurons were analyzed. A protocol that quantifies spine density and head diameter based on the Filament module of Imaris was used. The minimum end segment diameter (spine head) was set at ≥0.143 μm.

Slice Preparation. Rats were anesthetized with ketamine HCl (1 mg/kg Ketaset; Fort Dodge Animal Health) and decapitated. When necessary, head caps were removed first. The brain was removed from the skull, and coronal accumbens brain slices (220 μm) (VT1200S Leica vibratome; Leica Microsystems) were collected into a vial containing aCSF and a mixture of 5 mM kynurenic acid and 50 μM D-(-)-2-Amino-5-phosphonopentanoic acid (D-AP5). Slices were incubated at 32 °C for 30–40 min and then stored at room temperature.

In Vitro Whole-Cell Recording. All recordings were collected at 32 °C (TC-344B; Warner Instrument) in the dorsomedial NAcore. Inhibitory synaptic transmission was blocked with picrotoxin (50 μM). Multiclamp 700B (Axon Instruments) was used to record excitatory postsynaptic currents (EPSCs) in whole-cell patch-clamp configuration. Glass microelectrodes (1–2 MΩ) were filled with cesium-based internal solution (in mM: 124 cesium methanesulfonate, 10 Hepes potassium, 1 EGTA, 1 MgCl2, 10 NaCl, 2.0 MgATP, and 0.3 NaGTP, 1 QX-314, pH 7.2–7.3, 275 mOsm). Data were acquired at 10 kHz and filtered at 2 kHz using AxoGraph X software (AxoGraph Scientific). To evoke EPSCs a bipolar stimulating electrode (FHC) was placed ∼300 μm dorsomedial of the recorded cell to maximize chances of stimulating prelimbic afferents. The stimulation intensity chosen evoked a ∼50% of maximal EPSC. Recordings were collected every 20 s Series resistance (Rs) measured with a 2-mV depolarizing step (10 ms) given with each stimulus and holding current were always monitored online. Recordings with unstable Rs or when Rs exceeded 10 MΩ were aborted.

Measuring the AMPA/NMDA Ratio. Recordings started no earlier than 10 min after the cell membrane was ruptured, to allow diffusion of the internal solution into the cell. AMPA currents were first measured at −80 mV to ensure stability of response. Then the membrane potential was gradually increased until +40 mV. Recording of currents was resumed 5 min after reaching +40 mV to allow stabilization of cell parameters. Currents composed of both AMPA and NMDA components were then obtained. Then D-AP5 was bath-applied (50 μM) to block NMDA currents, and recording of AMPA currents at +40 mV was started after 2 min. NMDA currents were obtained by subtracting the AMPA currents from the total current at +40 mV.

Membrane Fractionation and Western Blotting. Crude membrane fractionation was prepared for assessment of change in protein expression. Animals were rapidly decapitated at $t = 0$, and NAcore tissue was dissected and homogenized. Homogenates were centrifuged at 1,000 × *g* for 10 min at 4 °C, and the pellet was homogenized with an additional 0.2 mL homogenization buffer and centrifuged again. Supernatants were centrifuged at 12,000 × *g* for 20 min. The resultant pellet was resuspended and supplemented with 1.0% SDS as well as protease and phosphatase inhibitors. Protein concentration was determined, and equal microgram quantities were loaded per lane. Corresponding antibodies were used, and Western blotting was performed onto nitrocellulose membranes. To maximize use of tissue, individual gel lanes were used to probe multiple proteins of different molecular weights. For the proteins in Fig. 5, 10–20 μg of protein was loaded in each lane. Calnexin was used as an unchanged loading control, and data were normalized to yoked saline controls (details in *SI Experimental Procedures*).

Statistics. All spine density and d_h data were statistically analyzed by averaging the values for all of the neurons in each animal. The number of determinations in each group was established using an analysis of statistical power based on previous data from our laboratory (9, 22). Behavioral data were analyzed using repeated-measures ANOVAs, and *t* tests were used to compare d_h and A/N. Post hoc comparisons were conducted using Bonferroni-corrected *t* tests. All statistical tests were conducted using Graphpad or SPSS software packages. Rats that did not meet criteria for acquisition of nicotine self-administration and/or extinguished lever pressing, or that had blocked guide cannulae before microinjection, were eliminated.

ACKNOWLEDGMENTS. We thank Drs. Haowei Shen, Michael T. Bardo, Rachel Smith, Michael Scofield, Robyn Brown, Sade Spencer, Matthew Feltenstein, and Joshua Beckmann for conceptual advice, and Charles Thomas for technical assistance. This work was supported by National Institutes of Health Grants DA007288 and DA033690 (to C.D.G.) and DA03906, DA012513, and DA015369 (to P.W.K.).

1. Koh HK, Sebelius KG (2012) Ending the tobacco epidemic. *JAMA* 308(8):767–768.
2. Shiffman S, Brockwell SE, Pillitteri JL, Gitchell JG (2008) Use of smoking-cessation treatments in the United States. *Am J Prev Med* 34(2):102–111.
3. Stolerman IP, Jarvis MJ (1995) The scientific case that nicotine is addictive. *Psychopharmacology (Berl)* 117(1):2–10, discussion 14–20.
4. Nides M (2008) Update on pharmacologic options for smoking cessation treatment. *Am J Med* 121(4, Suppl 1):S20–S31.
5. Mansvelder HD, Keath JR, McGehee DS (2002) Synaptic mechanisms underlie nicotine-induced excitability of brain reward areas. *Neuron* 33(6):905–919.
6. Picciotto MR, Addy NA, Mineur YS, Brunzell DH (2008) It is not "either/or": Activation and desensitization of nicotinic acetylcholine receptors both contribute to behaviors related to nicotine addiction and mood. *Prog Neurobiol* 84(4):329–342.
7. De Biasi M, Dani JA (2011) Reward, addiction, withdrawal to nicotine. *Annu Rev Neurosci* 34:105–130.
8. Mansvelder HD, McGehee DS (2002) Cellular and synaptic mechanisms of nicotine addiction. *J Neurobiol* 53(4):606–617.
9. Knackstedt LA, et al. (2009) The role of cystine-glutamate exchange in nicotine dependence in rats and humans. *Biol Psychiatry* 65(10):841–845.
10. Liechti ME, Lhuillier L, Kaupmann K, Markou A (2007) Metabotropic glutamate 2/3 receptors in the ventral tegmental area and the nucleus accumbens shell are involved in behaviors relating to nicotine dependence. *J Neurosci* 27(34):9077–9085.
11. Shen H, Moussawi K, Zhou W, Toda S, Kalivas PW (2011) Heroin relapse requires long-term potentiation-like plasticity mediated by NMDA2b-containing receptors. *Proc Natl Acad Sci USA* 108(48):19407–19412.
12. Shen HW, et al. (2009) Altered dendritic spine plasticity in cocaine-withdrawn rats. *J Neurosci* 29(9):2876–2884.

13. McFarland K, Lapish CC, Kalivas PW (2003) Prefrontal glutamate release into the core of the nucleus accumbens mediates cocaine-induced reinstatement of drug-seeking behavior. *J Neurosci* 23(8):3531–3537.
14. Epstein DH, Preston KL, Stewart J, Shaham Y (2006) Toward a model of drug relapse: An assessment of the validity of the reinstatement procedure. *Psychopharmacology (Berl)* 189(1):1–16.
15. LaLumiere RT, Kalivas PW (2008) Glutamate release in the nucleus accumbens core is necessary for heroin seeking. *J Neurosci* 28(12):3170–3177.
16. Park WK, et al. (2002) Cocaine administered into the medial prefrontal cortex reinstates cocaine-seeking behavior by increasing AMPA receptor-mediated glutamate transmission in the nucleus accumbens. *J Neurosci* 22(7):2916–2925.
17. Moussawi K, et al. (2011) Reversing cocaine-induced synaptic potentiation provides enduring protection from relapse. *Proc Natl Acad Sci USA* 108(1):385–390.
18. Matsuzaki M, Honkura N, Ellis-Davies GC, Kasai H (2004) Structural basis of long-term potentiation in single dendritic spines. *Nature* 429(6993):761–766.
19. Carlisle HJ, Kennedy MB (2005) Spine architecture and synaptic plasticity. *Trends Neurosci* 28(4):182–187.
20. De Roo M, Klauser P, Muller D (2008) LTP promotes a selective long-term stabilization and clustering of dendritic spines. *PLoS Biol* 6(9):e219.
21. Yang Y, Zhou Q (2009) Spine modifications associated with long-term potentiation. *Neuroscientist* 15(5):464–476.
22. Knackstedt LA, Melendez RI, Kalivas PW (2010) Ceftriaxone restores glutamate homeostasis and prevents relapse to cocaine seeking. *Biol Psychiatry* 67(1):81–84.
23. Cull-Candy S, Kelly L, Farrant M (2006) Regulation of Ca2+-permeable AMPA receptors: synaptic plasticity and beyond. *Curr Opin Neurobiol* 16(3):288–297.
24. Conrad KL, et al. (2008) Formation of accumbens GluR2-lacking AMPA receptors mediates incubation of cocaine craving. *Nature* 454(7200):118–121.
25. Cull-Candy SG, Leszkiewicz DN (2004) Role of distinct NMDA receptor subtypes at central synapses. *Sci STKE* 2004(255):re16.
26. Papouin T, et al. (2012) Synaptic and extrasynaptic NMDA receptors are gated by different endogenous coagonists. *Cell* 150(3):633–646.
27. Petralia RS (2012) Distribution of extrasynaptic NMDA receptors on neurons. *ScientificWorldJournal* 2012:267120.
28. Huang YH, et al. (2009) In vivo cocaine experience generates silent synapses. *Neuron* 63(1):40–47.
29. Cull-Candy S, Brickley S, Farrant M (2001) NMDA receptor subunits: Diversity, development and disease. *Curr Opin Neurobiol* 11(3):327–335.
30. Stitzer ML, Walsh SL (1997) Psychostimulant abuse: The case for combined behavioral and pharmacological treatments. *Pharmacol Biochem Behav* 57(3):457–470.
31. Badiani A, Belin D, Epstein D, Calu D, Shaham Y (2011) Opiate versus psychostimulant addiction: The differences do matter. *Nat Rev Neurosci* 12(11):685–700.
32. Gass JT, Sinclair CM, Cleva RM, Widholm JJ, Olive MF (2011) Alcohol-seeking behavior is associated with increased glutamate transmission in basolateral amygdala and nucleus accumbens as measured by glutamate-oxidase-coated biosensors. *Addict Biol* 16(2):215–228.
33. Gipson CD, et al. (2013) Relapse induced by cues predicting cocaine depends on rapid, transient synaptic potentiation. *Neuron* 77(5):867–872.
34. Zhou W, Kalivas PW (2008) N-acetylcysteine reduces extinction responding and induces enduring reductions in cue- and heroin-induced drug-seeking. *Biol Psychiatry* 63(3):338–340.
35. Ramirez-Nino AM, D'Souza MS, Markou A (2013) N-acetylcysteine decreased nicotine self-administration and cue-induced reinstatement of nicotine seeking in rats: Comparison with the effects of N-acetylcysteine on food responding and food seeking. *Psychopharmacology (Berl)* 225(2):473–482.
36. Sari Y, Sakai M, Weedman JM, Rebec GV, Bell RL (2011) Ceftriaxone, a beta-lactam antibiotic, reduces ethanol consumption in alcohol-preferring rats. *Alcohol Alcohol* 46(3):239–246.
37. Misra C, Brickley SG, Farrant M, Cull-Candy SG (2000) Identification of subunits contributing to synaptic and extrasynaptic NMDA receptors in Golgi cells of the rat cerebellum. *J Physiol* 524(Pt 1):147–162.
38. Kash TWD (2007) NMDAR LTP and LTD induction: 2B or Not 2B... is that the question? *Debates Neurosci* 1:79–84.
39. Anderson SM, et al. (2008) CaMKII: A biochemical bridge linking accumbens dopamine and glutamate systems in cocaine seeking. *Nat Neurosci* 11(3):344–353.
40. Grueter BA, Robison AJ, Neve RL, Nestler EJ, Malenka RC (2013) ΔFosB differentially modulates nucleus accumbens direct and indirect pathway function. *Proc Natl Acad Sci USA* 110(5):1923–1928.
41. Paxinos G, Watson C (2007) *The Rat Brain in Stereotaxic Coordinates* (Academic/Elsevier, Amsterdam), 6th Ed.